Assessment of GAFF2 and OPLS-AA general force fields in combination with the water models TIP3P, SPCE and OPC3 for the

Assessment of GAFF2 and OPLS-AA general force fields in combination with the water models TIP3P, SPCE and OPC3 for the solvation free energy of drug-like organic molecules

Dario Vassetti, Marco Pagliai, and Piero Procacci*

Department of Chemistry, University of Florence, Via Lastruccia n. 3, Sesto Fiorentino, I-50019 Italy

E-mail: procacci@unifi.it

Abstract

Molecular dynamics simulations have been performed to compute the solvation free energy and the octanol/water partition coefficients for a challenging set of selected organic molecules, characterized by the simultaneous presence of functional groups coarsely spanning a large portion of the chemical space in drug-like compounds and, in many cases, by a complex conformational landscape (2-propoxyethanol, acetylsalicylic acid, cyclohexanamine, dialifor, ketoprofen, nitralin, profluralin, terbacil). OPLS-AA and GAFF2 parameterizations of the organic molecules and of 1-octanol have been done via the web-based automatic parameter generators, LigParGen [Dodda et al. Nucl. Acids Res. 2017; 121, 3864] and PrimaDORAC [Procacci, J. Chem. Inf. Model. 2017; 57, 1240], respectively. For the water solvent, three popular three-point sites models, TIP3P, SPCE and OPC3, were tested. Solvation free energies in water and 1-octanol are evaluated using a recently developed non equilibrium alchemical technology

[Procacci et al. J. Chem. Theory Comput. 2014; 10, 2813]. Extensive and accurate simulations including all possible combinations of organic molecule, solvent and solvent model, allowed to assess the accuracy with regard to solvation free energies of the latest release of two widespread force fields, OPLS and GAFF. The collected data are relevant in the evaluation of the predictive power of these classical force fields (and of the related support software for automated parameterization) with regard to binding free energies in drug-receptor system for industrial applications.

Introduction

In silico profiling and characterization of potentially active compounds for pharmaceutical applications is probably one of the most challenging ongoing cooperative project in modern computational chemistry, involving an intense effort from both the academia and industrial players (see for example the worldwide DR3[1–3] blind challenges launched on a yearly basis and sponsored by important industrial partners). In recent years, exploiting the tumultuous growth and availability of computer power at affordable economical costs, several advanced computational techniques and tools, running on massively parallel high performing computing platforms (HPC), have been devised for the prediction of binding free energies in drug design and discovery projects.[4–9] Many of these modern computational technologies rely on a realistic representation of the biological target, based on the so-called all-atom model, whereby all the players in the system, including solvent molecules, proteins, substrates and drugs, interact via an atom-based potential function including two-body non bonded terms and up to four-body valence terms, ideally parameterizing the ground state Born-Oppenheimer multidimensional surface spanned by the many-body system in standard conditions. At the heart of this complex parameterization, which is common to traditional docking, molecular mechanics (MM) approaches as well as to Molecular Dynamics (MD) advanced techniques, are the so-called general *force fields*,[10–12] i.e. representational and, in principle, transferable protocols for the atom-atom interactions of any kind of molecular

system acting as a drug or as a substrate in biologically relevant applications.

In this paper we analyze the performances of the latest variant of two of the most important force fields currently developed for pharmaceutical relevant molecules, namely the Optimized Potentials for Liquid Simulation (OPLS-AA[11]) and the General AMBER Force Field (GAFF2[13]). The assessment is done using a well established benchmark based on the calculations of the solvation free energies. The parameterizations of the selected solute molecules is provided by the recently developed web-based automatic parameter generators, LigParGen[14] for OPLS-AA and PrimaDORAC[15] for GAFF2.

The centrality of accurate solvation free energies in computational drug design can be easily grasped by considering that the binding free energy of drug-like molecule towards a protein target may be viewed[16–18] as the difference in the solvation free energies of the compound when embedded in two distinct environments, i.e. in the bulk solvent and in the protein hydrophobic pocket hosting the bound drug.

For our assessment, we have selected eight organic molecules, taken from the database commendably compiled by Mobley *et al*,[19] which are not usually employed in the training sets for force field refinement,[11] either due to their chemical complexity (with the simultaneous presence of disparate chemical moieties) or because of their intrinsic enhanced flexibility spanning competitive meta-stable conformational states. For these molecules, accurate experimental data are available[19–21] as well as theoretical data on hydration free energies done using older versions of the GAFF force field.[19]

The other key aspect in solvation free energy evaluation concerns of course the solvent and solute-solvent interaction model. In this regard, the accurate modeling of explicit water solvent is indeed a crucial ingredient in any computational all-atoms approach of biological systems. A reliable water model must be, at the same time, simple enough to be computationally affordable and capable of reproducing the key chemical-physical properties of the liquid, such as the dielectric screening and mass density, that are crucial in the thermodynamic balance of the non covalent association in condensed phases. In this paper we have

used, in combination with the two cited general force fields, three commonly adopted simple three sites water models, namely the Transferable Inter-molecular Potential with 3 Point (TIP3P)[22] which accurately reproduces the dielectric constant at 300 K underestimating the density of liquid, the SPCE (Extended Simple Point Charge[23]), producing a correct density and a somewhat lower dielectric constant, and finally the recently developed OPC3 or 3-point Optimal Point Charge model[24] (see Table 1 further on).

Behavior of the force fields when the selected molecules are immersed in an hydrophobic environment has been assessed using, as a representative solvent, 1-octanol. Solvation properties in this solvent are frequently determined for predicting the tendency of the compounds to cross biological membranes.[20] For the modeling of liquid 1-octanol in standard conditions with GAFF2 and OPLS-AA, we have adopted the corresponding PrimaDORAC and LigParGen generated parameterizations.

We have performed extensive molecular dynamics simulations of all possible 64 combinations of organic molecule, general force fields, solvent (water/octanol) and water model. The methodology for computing the solvation free energies is based on the recently developed fast switching annihilation (FSAM) method.[25,26] The approach is in essence a nonequilibrium (NE) variant of the Free Energy perturbation[27] (FEP) or Thermodynamic integration[28] (TI) traditional equilibrium technologies for alchemical[16] free energy calculations. NE alchemy computes the free energy in three distinct and consecutive computational tasks: in the first task, the fully coupled end state of the system is canonically sampled using the Hamiltonian Replica Exchange method (HREM).[29] In the second task, starting from the canonical states sampled in the preceding task, a swarm of fast and independent (non communicating) NE annihilation trajectories are launched in parallel, producing eventually an annihilation work distribution. In the third task, the work distribution obtained in the second step is used to evaluate the corresponding free energy exploiting the Crooks theorem for normal distribution[30,31] or for Gaussian mixtures.[32] As such, NE alchemy is specifically tailored for an efficient implementation on modern HPC facilities with non uniform memory access,

based on a multilevel parallelism allowing to produce, for the system under scrutiny, a total simulation of 0.3 μs in few tens of minutes.[33]

This paper is organized as follows. In Section 2, we provide the methodological details of each of the computational steps involved in NE alchemy. In Section 3, results for solvation energies for the eight selected molecules using the OPLS-AA and GAFF2 force fields and the OPC3, SPCE and TIP3P water models are presented and critically analyzed in terms of correlation coefficients and mean unsigned errors between experimental and theoretical data. Conclusive remarks are finally discussed in Section 4.

Methods

In Figure 1, we show the set of eight organic molecules that were selected in order to compute the solvation free energies for all possible combinations of force field and solvent model (six for the hydration energies and two for the solvation energy in 1-octanol).

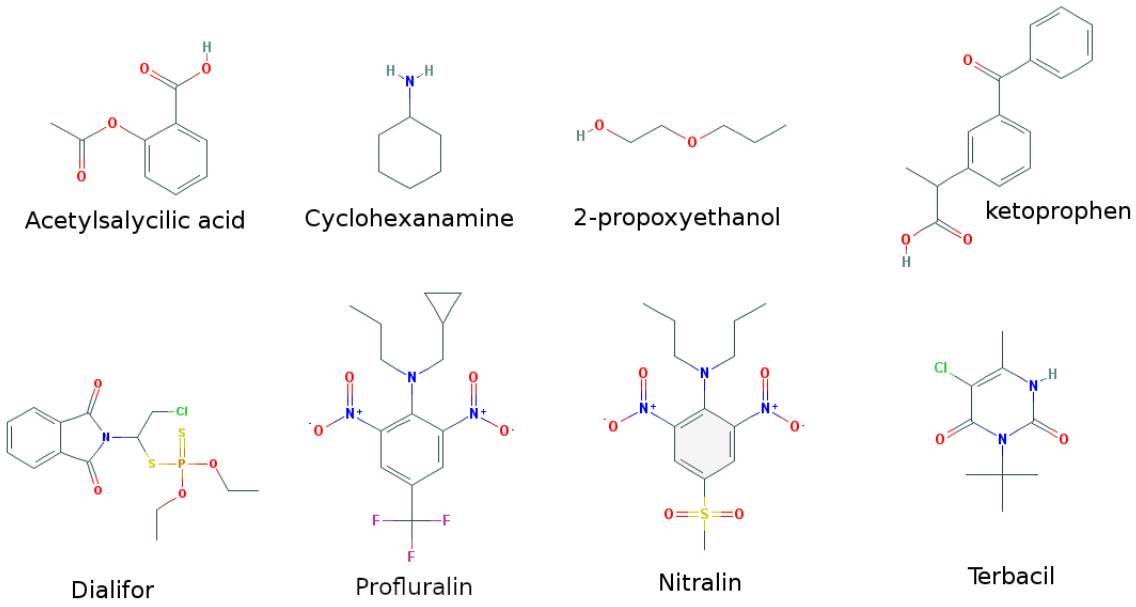

Figure 1: Selected set of molecules

Some of the selected molecules (nitralin, profluralin, terbacil, dialifor) are characterized

by the simultaneous presence of functional groups spanning a large portion of the chemical space in drug-like compounds and virtually all of them exhibit, to some extent, a challenging conformational landscape (e.g. boat/chair conformational distribution in cyclohexanamine, incidence of intramolecular H-bond in acetylsalicylic acid and 2-propoxyethanol, and, in most cases, abundance of rotable bonds and competitive conformations). In the development of general force fields, transferable atomic types and charge evaluation protocols, like the 1.14*CM1A and 1.14*CM1A-LBCC[11] or the AM1/BCC,[34] are refined using restricted sets of molecules, usually indicated as the training sets, typically including a single specific chemical moiety (e.g. halogen, carboxy, amino, amide etc.) in combination with a relatively simple common molecular scaffolds (e.g. phenyl, naphtyl, butyl etc.).[11,13] As the selected eight molecules were not, in general, included in the training set used for OPLS-AA[11]or GAFF2,[35] the computation of their solvation free energies constitutes a significant challenge for a quantitative assessment of the accuracy of these force field. For all the selected molecules, experimental data of the hydration free energies[19] and of the octanol/water partition coefficients (LogP)[21] have been reported.

General setup of the simulations

The OPLS-AA and GAFF2 parameterization of the molecules of Figure 1 have been done by using the automatic web-based parameter generators LigParGen[14] and PrimaDORAC,[15] respectively. These software tools typically provide, upon input of the molecular structure and net charge, the topological and parameter files needed in MM or MD simulations. These files are often given in various format so that they can be used directly as input files for common simulation packages.[12,33,36,37] For LigParGen, the SMILES[38] files were used as input with the default setup. For PrimaDORAC, the default setup provided by the web interface was used by uploading the canonical OpenBabel[39] generated PDB file from the SMILES file. In the Supporting Information, the full archive of the LigParGen and PrimaDORAC generated topological and parameter files for the eight selected molecules is provided as a

compressed archive (file `tpgprm.zip`).

The parameterization of the explicit water solvent in hydration free energy calculations is done using the TIP3P,[22] OPC3[24] and SPCE[23] three-point site models. The salient chemical-physical properties of these three models for liquid water have been extensively reported elsewhere[23,24] and are summarized in Table 1. Although still not commonly adopted with respect to TIP3P and SPCE, the OPC3 model appears to reproduce with greater accuracy the chemical-physical properties of the liquid that are crucial in hydration free energy calculations, namely the mass density and the dielectric constant.

Table 1: TIP3P, SPCE and OPC3 water model main characteristics: $q(e)$ hydrogen charge; μ dipole moment; l O-H Bond length; θ HÔH Angle; σ, ϵ Lennard-Jones oxygen-oxygen potential parameters; ρ density at P=1 atm and T=298 K; ϵ_{diel} dielectric constant at P=1 atm and T=298 K (data taken from Ref.[24])

model	q (e)	μ (D)	l (Å)	θ (°)	σ (Å)	ϵ (kJ/mol)	ρ (g/cm^3)	ϵ_{diel}
TIP3P	0.417	2.35	0.9572	104.52	3.15061	0.6364	0.980	94
SPCE	0.4238	2.35	1.0	109.47	3.166	0.65	0.994	68
OPC3	0.447585	2.43	0.97888	109.47	3.17427	0.68369	0.995	78

For the parameterization of 1-octanol as a solvent, we have adopted the corresponding PrimaDORAC (for GAFF2) and LigParGen (for OPLS-AA) parameterizations. Solvent (water and 1-octanol) topological and parameter files are reported in the archive `tpgprm.zip` provided in the Supplementary Information.

All solute molecules were considered in their neutral form including those with acid carboxylic or basic amino moieties. In fact, experimental hydration free energies and LogP coefficients are normally referred to the un-ionized species. Solvation free energy were evaluated by dissolving the selected solutes in about 1000 water molecules or 125 molecules of octanol in a cubic MD box. All simulations were done in the NPT isothermal-isobaric ensemble, yielding a mean side-length around 32-33 Å in both water and 1-octanol. The external pressure was set to 1 atm using a Parrinello-Rahman Lagrangian[40] with isotropic stress tensor while temperature was held constant at 300 K using three Nosé Hoover-thermostats

coupled to the translational degrees of freedom of the systems and to the rotational/internal motions of the solute and of the solvent. The equations of motion were integrated using a multiple time-step r-RESPA scheme[41] with a potential subdivision specifically tuned for bio-molecular systems in the NPT ensemble.[40,42] The long range cut-off for Lennard-Jones interactions was set to 13 Å in all cases. Long range electrostatic were treated using the Smooth Particle Mesh Ewald method,[43] with an α parameter of 0.37 $Å^{-1}$, a grid spacing in the direct lattice of about 1 Å and a fourth order B-spline interpolation for the gridded charge array. All calculations were done using the program ORAC.[33] The ORAC code, including the source, can be freely downloaded from the site http://www.chim.unifi.it/orac.

Fast Switching annihilation method (FSAM) for the hydration free energy

The theoretical background of the FSAM (or FSDAM, Fast Switching double annihilation method) alchemical methodology has been thoroughly described elsewhere.[25,26,33,44–47] Here we briefly summarize the salient technical aspects of FSAM as long as solvation free energy calculations are concerned.

As outlined in the Introduction, the method can be divided in two main computational stages and one straightforward post-analysis step. First, the canonical conformational states of the solvated, fully coupled solute are sampled using Hamiltonian Replica Exchange with torsional tempering (HREM-TT stage).[48,49] In the second step, starting from these initial states, the solute is rapidly annihilated in a swarm of independent NE trajectories producing eventually an annihilation work distribution. Finally, the character of the work distribution is examined using standard normality tests, like the Anderson Darling test[50–52] (ADT) and the solvation free energy is recovered by exploiting the Crooks theorem[53] for normal distribution[30,31] or, in case of ADT failure, for mixture of normal distributions.[32]

The scaling protocol in the HREM-TT equilibrium stage is illustrated in the left panel of Figure 2 where we show, as an example, the distribution of the torsional energy, referred to

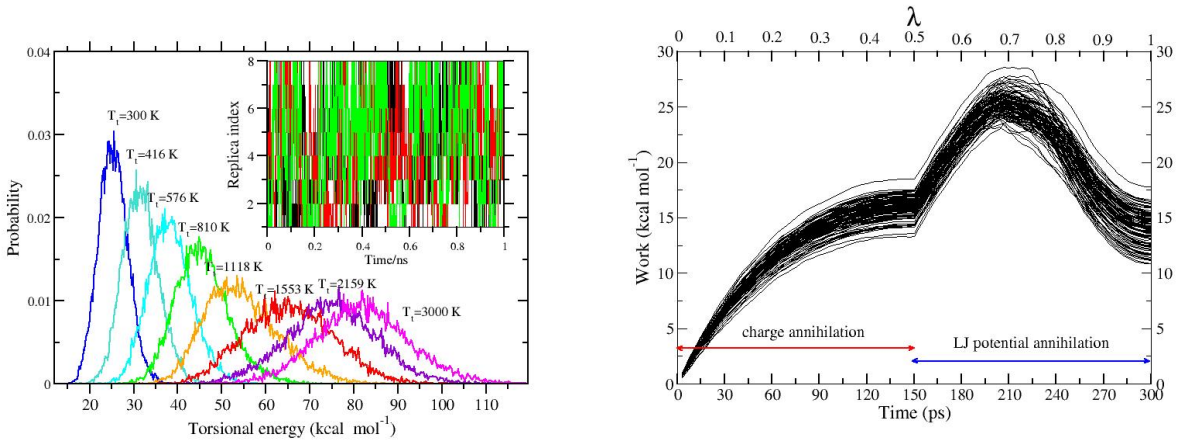

Figure 2: Left panel: Distribution of the torsional energy in GAFF2 Dialifor in OPC3 water in the H-REM torsional tempering simulation; in the inset three representative walkers in the GE space are shown. Right panel: Time record of the work during one hundred fast (300 ps) non equilibrium annihilation trajectories of GAFF2 Dialifor in OPC3 water.

dialifor in OPC3 water, in each of the eight replicas. Exchanges are attempted every large time steps[54] (15 fs). In water, torsional tempering involves only the solute with the hottest '"torsional temperature" corresponding to 3000 K (lowest scaling factor of 0.1). The overlap of contiguous (unscaled) torsional energy distributions in water is substantial yielding an acceptance ratio above 50%. In octanol, torsional tempering involves the solute and the solvent as well. In this case, in order to have a significant acceptance ratio[49] with 8 replicas, the maximum torsional temperature is reduced to 1000 K (lowest scaling factor of 0.3). The HREM-TT simulation lasted, in all 64 cases, about 8 ns (target replica), hence producing a total simulation time of 4 μs *circa*. The whole calculation required about 60000 core hours (mean parallel job size of 500-600 cores) running mostly on the A1-Broadwell partition at the CINECA HPC,[55] and was completed in few wall clock days with normal HPC workload.

In the right panel of Figure 2, the second computational step of FSAM in a representative case is demonstrated by reporting the annihilation work during the progress of the λ alchemical solute decoupling coordinate for a swarm of NE trajectories. The number of NE trajectories is 532 for all 64 possible FSAM simulations. In water, the annihilation time ($\lambda = 1$) is set to $\tau = 300$ ps while in octanol we set $\tau = 600$ ps. These two different annihila-

tion rates are a consequence of the different behavior of the dissipation in the NE alchemical decoupling in the two solvents. The dissipated work $W_{\mathrm{d}} = \langle W \rangle - \Delta G$, for Gaussian work distributions, can be straightforwardly estimated[56] from the variance, i.e. $W_{\mathrm{diss}} = \frac{1}{2}\beta\sigma^2$. As shown in the Supporting Information (Table S1 and Table S3), the selected annihilation times produce similar mean dissipation in the two solvents. On the other hand, these annihilations times (as also shown in Figure S9 of the Supporting information where the behavior of the NE work was analyzed as a function of the annihilation time τ) allow to obtain accurate estimate of the hydration free energies.[25] The annihilation protocol of the τ lasting NE processes was common to all 64 FSAM simulations and stipulates that the electrostatic interactions between the solute and the environment are linearly brought to zero at $t = \tau/2$, while the Lennard-Jones interactions are switched off in the range $\tau/2 < t < \tau$ using a soft-core Beutler potential[57] regularization as λ is approaching to one.

The FSAM-NE stage produced a total simulation time of 10 μs *circa*. The whole calculation required about 102000 core hours (mean parallel job size of about 3000 cores) running on the A1-Broadwell partition at the CINECA HPC[55] and on the CRESCO6 cluster,[58,59] and was completed in few tens of wall-clock hours with normal HPC workload.

In the example reported in the right panel of Figure 2, we can see that the alchemical work rapidly grows during the discharging process; then it continues to grow reaching a maximum when approximately half of the Lennard-Jones interactions had been switched off. From now on, with solvent filling the volume left free by the annihilating solute, there is a substantial energy gain corresponding to minus the work to form the cavity in the solvent. This trend in the annihilation work is common to all molecules, irrespective of the solvent and force field combination.

Gaussian mixture free energy estimates

In principle, the collection of NE work values acquired in the FSAM stage (Figure 2, right panel) could be used to estimate the solvation free energy via the Jarzysnki exponential

average,[60] namely $e^{-\beta\Delta G} = \langle e^{-\beta W} \rangle$. Exponential averages, on the other hand, critically depend on values sampled in left tail of the distribution, i.e. a statistics that is both inherently noisy and biased, even if the spread of the work data is only moderately larger than $k_B T$.[30,61–63] Actually, if the work distribution is normal or is given by a mixture of normal components, an unbiased and accurate estimate can be straightforwardly derived by exploiting the Crooks theorem.[30,31,46,47] The character of the distribution can be instantly[47] assessed by performing the Anderson-Darling test[50] for normality. The latter is defined via the quantity $A^2 = \sum_{i=1}^{n} \frac{2i-1}{n} [\ln(\Phi(w_i) + \ln(1 - \Phi(w_{n+1-i})]$, where Φ is the Gaussian cumulative distribution function with sample mean and variance and w_i are the work values sorted in ascending order. Among the *plethora* of normality tests,[52,64] in recent FSDAM studies,[46,47] the ADT was chosen precisely for its sensitivity to the tails.[64] In case of a positive ADT, the Crooks theorem allows to straightforwardly recover[31] the solvation free energy from the mean and variance of the distribution as

$$\Delta G = \langle W \rangle - \frac{1}{2} \beta \sigma^2 \tag{1}$$

If the ADT fails, a mixture of N_g normal components is assumed, with N_g being determined by examining the third (skewness) and fourth (kurtosis) standardized moments of the distribution,[47] namely $N_g = 2$ if either skewness or kurtosis are present and $N_g = 3$ if both are present. The parameters of the N_g mixture are determined using the Expectation-Maximization (EM) algorithm.[65] Exploiting again the Crooks theorem, the solvation free energy can be evaluated as[32,46,47]

$$\Delta G = -RT \ln \left[\sum_{i}^{N_g} w_i e^{-\beta(\mu_i - \frac{1}{2}\beta(\sigma_i^2)} \right] \tag{2}$$

where μ_i, σ_i are the mean and variance of the i-th component of the mixture (determined via EM) and with the weights satisfying $\sum_i w_i = 1$. In the Figure 3, we show two examples of work distribution obtained in the fast annihilation stage of the solute. The distributions

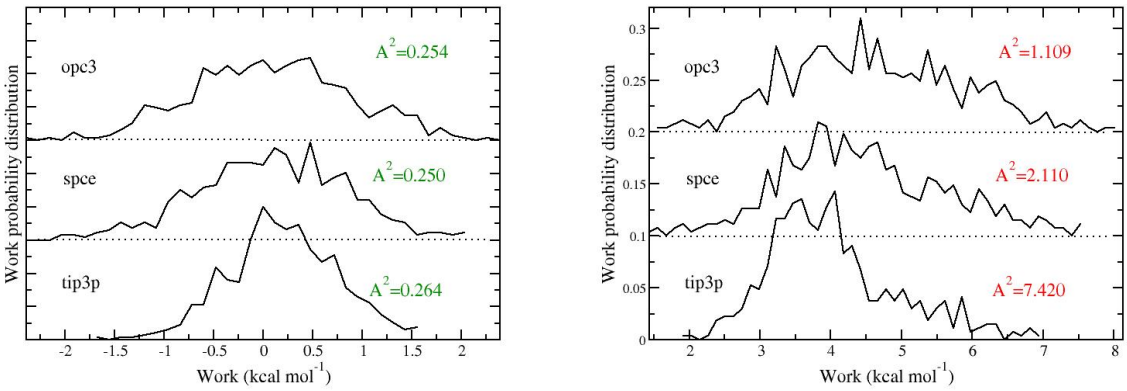

Figure 3: Left panel: Work distribution for cyclohexanamine with GAFF2. Right panel: Work distribution for 2-propoxyethanol with OPLS-AA. The critical value of ADT at the level $\alpha = 0.05$ is 0.752.[51]

on the left (cyclohexanamine in water with GAFF2) are all Gaussian according to the ADT. Those on the right (2-propoxyethanol in water with OPLS-AA) are visibly non symmetric largely failing the ADT. The OPLS-AA/TIP3P distribution, for example, according to the moments reported in Table S2 of the Supporting Information, is positively skewed and exhibits a marked platykurtic behavior. Full data on all the computed 64 work distributions, including mean, variance, skewness, kurtosis and A^2 for each combination in water and octanol, are provided in the Supporting Information (section "Work distribution data"). Errors on the solvation free energies, Eq. 1 or Eq. 2, can be straightforwardly computed using bootstrap with re-sampling.[66] The work distributions in water were found normal in 33 cases out of 48 (see Table S1 in the Supporting Information). In 1-octanol all work distributions are found normal, except for that of 2-propoxy-ethanol using the OPLS-AA force field (Table S3 in the Supporting Information).

Results and Discussion

Conformational analysis in water from the REM equilibrium stage

The conformational landscape and entropy of a flexible drug-like compound in bulk water is a key property in shaping its affinity for a target protein. Since the drug is in general frozen in one single conformation when bound to the protein, the conformational entropy loss upon binding always constitutes a penalty for the binding affinity.[18] In Table 2, we have reported the mean gyration radius (MGR) for the selected molecules sampled at the target state in the H-REM simulation using all possible force field/water model combination. Expectedly, for a given force field, MGR's are quite insensitive to the adopted water model.

Table 2: Mean gyration radius (MGR) (in Å) in water solution for the selected set of molecules using the combination OPLS/GAFF force fields and OPC3/SPCE/TIP3P three site water model. The I_m (in u.m.a. see text) entries refer to the molecular charge strength.

	GAFF2				OPLS-AA			
	I_m	MGR			I_m	MGR		
		OPC3	SPCE	TIP3P		OPC3	SPCE	TIP3P
2pro	0.042	2.55± 0.10	2.54± 0.10	2.55± 0.10	0.046	2.60± 0.12	2.63± 0.11	2.59± 0.12
acet	0.143	2.92± 0.04	2.91± 0.04	2.92± 0.04	0.088	3.01± 0.04	3.01± 0.04	3.01± 0.04
cycl	0.023	2.17± 0.04	2.18± 0.04	2.18± 0.04	0.075	2.11± 0.02	2.13± 0.05	2.11± 0.02
dial	0.095	4.01± 0.27	4.00± 0.22	4.07± 0.27	0.287	4.58± 0.15	4.55± 0.13	4.59± 0.15
keto	0.075	3.76± 0.17	3.74± 0.17	3.77± 0.18	0.054	3.80± 0.17	3.81± 0.18	3.79± 0.17
nitr	0.127	3.82± 0.07	3.82± 0.07	3.81± 0.06	0.155	3.79± 0.06	3.81± 0.06	3.81± 0.06
prof	0.061	3.57± 0.07	3.58± 0.06	3.57± 0.07	0.095	3.56± 0.06	3.57± 0.06	3.57± 0.06
terb	0.069	3.08± 0.02	3.08± 0.02	3.08± 0.02	0.142	3.09± 0.02	3.09± 0.02	3.09± 0.02

Quite surprisingly, on the other hand, OPLS-AA and GAFF2 yield, in some cases, MGR's that are somewhat different due to a correspondingly different conformational behavior. If for acetylsalicylic acid and 2-propoxyethanol, OPLS-AA and GAFF2 exhibit deviations in the MGR of the order of 2%-3%, for dialifor OPLS-AA produces a MGR that is more than 10% higher than that obtained with GAFF2, largely exceeding the corresponding fluctuations. Further details on the conformational landscape are provided in the Supporting Information.

As shown in Figure S1, for example, in 2-propoxyethanol, the intramolecular H-bond involving the oxy moiety is shorter and stronger in GAFF2. In acetylsalicylic acid (Figure S2), OPLS-AA strongly disfavors, with respect to GAFF2, the formation of the intramolecular H-bond between the oxy oxygen and the proton of the carboxy group. In dialifor (Figure S4), the extended structure, with the propoxy far from the isoindol moiety, is by far the more stable conformer according to OPLS-AA, while GAFF2 predicts equal stability for the bend and extended structures. These different conformational behavior in water can be in part explained by evaluating the molecular charge strength, $I_m = \frac{1}{n}\sum_{i=1}^{n} q_i^2$ according to the two force fields (see Table 2). In dialifor, OPLS-AA has a much larger I_m, hence favoring the hydration of the highly charged atoms on the PO_2S_2 group and disfavoring structures stabilized by intrasolute hydrophobic interactions. For acetylsalicilic acid, the situation is reversed with the polar oxygen and hydrogen atoms bearing a higher charge in GAFF2, hence stabilizing the intramolecular hydrogen bond. The higher stability of the H-bond in GAFF2 for 2-propoxyethanol is likely due to the van der Waals modeling as the charges on O and H atoms are similar in the two force fields.

Discharging and dispersive-repulsive contributions to the solvation free energies

As it can be seen in the example of Figure 2 (right), the annihilation work of the solute can divided in two components, namely a steadily growing discharging work, when the atomic charges on the molecule are brought to zero at $\lambda = 0.5$, and a dispersive-repulsive annihilation work, when also the solute-solvent Lennard-Jones interaction are switched off at $\lambda = 1$. Correspondingly, using either Eq. 1 or Eq. 2 depending on the character of the corresponding distributions, one can compute a discharging and a dispersive-repulsive contribution to the solvation free energy, $\Delta G_q(\lambda = 0.5)$ and $\Delta G_{\mathrm{LJ}} = \Delta G - \Delta G_q$, respectively.

Water. In Figure 4 we show the correlation plot of ΔG_q (left) and ΔG_{LJ} (right) for the two force fields using the three water model. The discharging free energy, ΔG_q (left panel),

is remarkably insensitive to the adopted water model. OPLS-AA and GAFF2 data, on the other hand, do not appear to be strongly correlated ($R^2 = 0.69$). In four cases, in particular, OPLS-AA produces a ΔG_q significantly higher than that of GAFF2 (cycl, dial, prof); in one case (terbacil), ΔG_q is larger with GAFF2. For cyclohexanamine, dialifor and profluralin these discrepancies can be explained with the larger charge strength I_m (see Table 2) in OPLS-AA. For terbacil, while I_m is sensibly higher with OPLS-AA, the OPLS-AA charges on the solvent exposed carbonyl oxygen atom are smaller with respect to those of GAFF2, very likely indicating that these atomic charges play the major role in the hydration of the molecule.

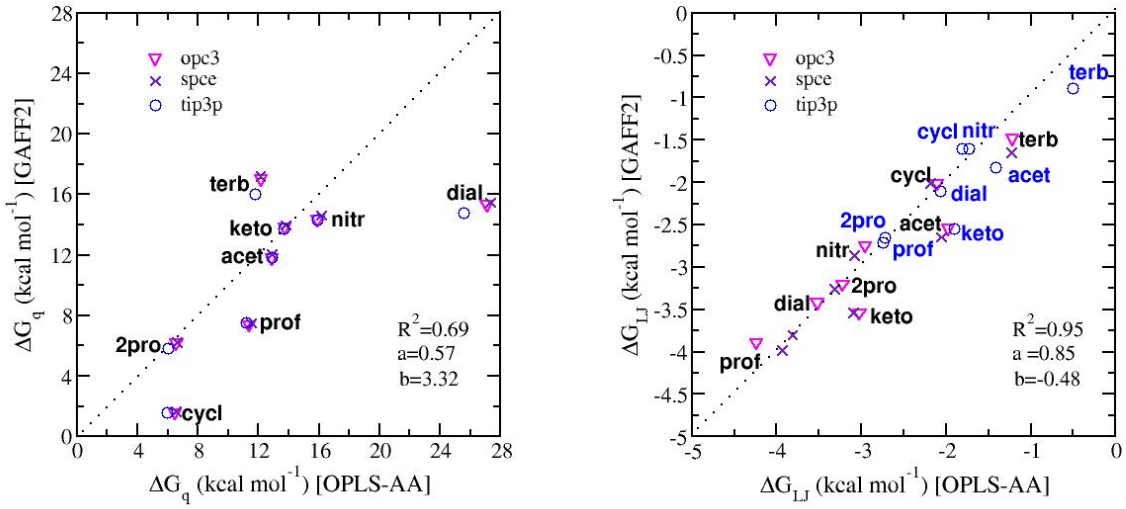

Figure 4: Correlation diagram OPLS-AA/GAFF2 for the discharging and dispersive-repulsive contributions (see text) to the hydration free energies using OPC3, SPCE and TIP3P water models. The overall Pearson correlation coefficient OPLS2/GAFF, R^2, along with slope and intercept of the best fitting line, a, b are also reported

As to the dispersive-repulsive contribution, ΔG_{LJ} (right panel), the two force fields predict a negative sign and yield highly correlated results. There are in this case significant differences in the ΔG_{LJ} depending on the adopted water model. ΔG_{LJ} values for TIP3P in particular, while preserving the strong correlation between the two OPLS-AA and GAFF2 force fields, are noticeably less negative with respect to those obtained with the OPC3 and

SPCE models. This is likely to be ascribed to the lower mass density exhibited by the TIP3P model (see Table 1) that correspondingly brings about a smaller energy gain when filling the solute cavity.

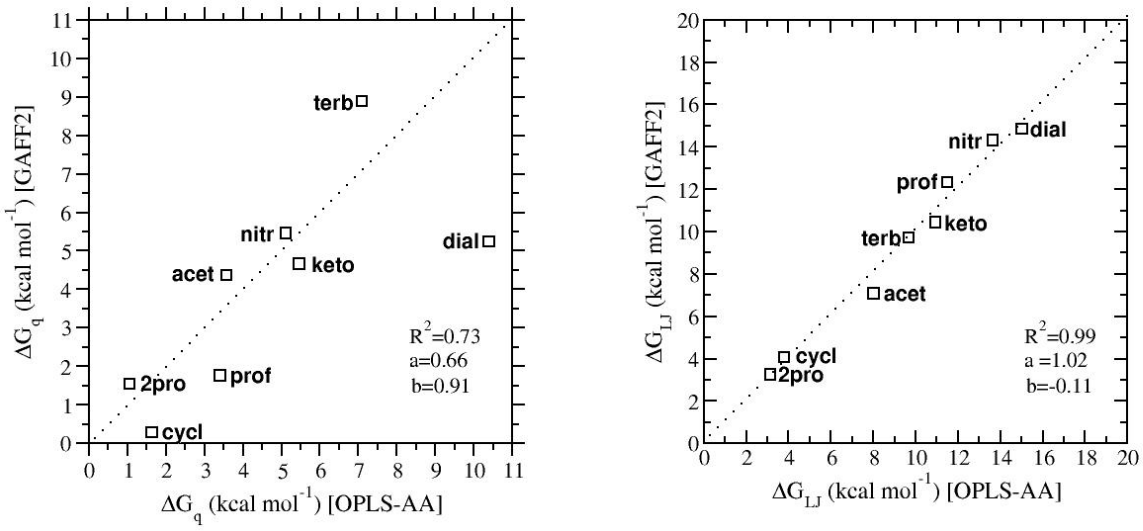

Figure 5: Correlation diagram OPLS-AA/GAFF2 for the discharging and dispersive-repulsive contributions (see text) to the solvation free energies in 1-octanol. The overall Pearson correlation coefficient OPLS2/GAFF, R^2, along with slope and intercept of the best fitting line, a, b are also reported

1-Octanol. In Figure 5, we show the OPLS-AA/GAFF correlation diagram for ΔG_q and $\Delta G_{\rm LJ}$ in 1-octanol. The pattern is similar to that observed in water. Also in the case of 1-octanol, we observe a strong OPLS-AA/GAFF2 correlation for dispersive-repulsive contribution, $\Delta G_{\rm LJ}$, and a weaker correlation for the discharging free energy ΔG_q. As observed in water, also in 1-octanol OPLS-AA yields, with respect to GAFF2, a larger ΔG_q for cyclohexanamine, dialifor and profluralin and smaller one for terbacil. Contrarily to what happens in water, $\Delta G_{\rm LJ}$ is positive in 1-octanol, with the negative cavity work not being able to compensate the free energy loss involved in switching off the Lennard-Jones interactions. In general OPLS-AA and GAFF2 produce similar results for $\Delta G_{\rm LJ}$, with the higher values observed for the more bulky molecules.

The comparison of the discharging and dispersive-repulsive component of the solvation

free energies in water and 1-octanol can provide valuable clues for a rationalization of the binding affinity of a small molecule for a protein target. As stated in the introduction, the binding free energy can be viewed as the difference of the solvation energy of the solute in two environment, namely that surrounding the solute in the bound state with a marked hydrophobic character, and the bulk water. According to Figure 4(left) and Figure 5(left), in bulk water, the discharging free energy ΔG_q for any given solute molecule is substantially larger than the corresponding ΔG_q in the mostly hydrophobic solvent 1-octanol. The dispersive-repulsive free energy ΔG_{LJ}, on the other hand, has an opposite behavior, being substantially larger in 1-octanol with respect to water (where is negative in all cases) for all solutes (see Figure 4, right panel and Figure 5, right panel). The differences $\Delta\Delta G_{\mathrm{LJ}}$ and $\Delta\Delta G_q$ for the water/1-octanol environments have hence, in general, opposite signs. The same situation can occur[33,45,46] in shaping the protein-drug dissociation free energy, that, in the case of binding driven by hydrophobic interactions, results from a differences between a *positive* solute dispersive-repulsive contribution $\Delta\Delta G_{\mathrm{LJ}} = \Delta G_{\mathrm{LJ\ bound}} - \Delta G_{\mathrm{LJ\ bulk}}$ favoring the binding and by a *negative* contribution due to the discharging process of the solute, namely $\Delta\Delta G_q = \Delta G_{q\ \mathrm{bound}} - \Delta G_{q\ \mathrm{bulk}}$.

Solvation free energy

In Table 3 we report the calculated hydration free energies of the eight selected molecules, using the GAFF2 and OPLS-AA general force fields in combination with the OPC3, SPCE and TIP3P models. Free energy estimates have been done using Eq. 1 or Eq. 2, depending on the number of normal components in the work distribution. Full details of the work distributions (including ADT, mean, variance, skewness and kurtosis) are reported in Tables S1 and S2 of the Supporting Information.

Table 3: Solvation free energies (kcal mol^{-1}) in water obtained with OPLS-AA and GAFF2 in combination with the three water models OPC3,SPCE, TIP3P. N_g is the number of normal components in the corresponding work distribution. For $\Delta G_{\rm calc}$, when $N_g = 1$ and $N_g > 1$, Eq. 1 and Eq. 2 are used, respectively. The error has been calculated using bootstrap with resampling.[66] The experimental values for the hydration free energies (kcal mol^{-1}) are taken from Ref.[19]

	GAFF						
	OPC3		SPCE		TIP3P		
Molecule	$\Delta G_{calc.}$	N_g	$\Delta G_{calc.}$	N_g	$\Delta G_{calc.}$	N_g	$\Delta G_{\rm exp}$
2pro.	-2.96 ±0.13	1	-3.00 ±0.14	2	-3.24 ±0.59	3	-6.40±0.60
acet.	-9.29 ±0.27	1	-9.37 ±0.24	2	-10.02 ±0.13	1	-9.94±0.18
cycl.	0.44 ±0.09	1	0.41 ±0.09	1	0.06 ±0.07	1	-4.59±0.60
dial.	-11.96 ±0.22	1	-11.04 ±0.65	2	-12.67 ±0.20	1	-5.74±1.93
keto.	-10.49 ±0.44	2	-10.28 ±0.44	2	-10.54 ±0.57	2	-10.78±0.18
nitr.	-11.64 ±0.21	1	-11.75 ±0.21	1	-12.72 ±0.12	1	-7.98±1.93
prof.	-3.49 ±0.23	1	-3.46 ±0.18	1	-4.79 ±0.13	1	-2.45±1.37
terb.	-15.64 ±0.16	1	-15.40 ±0.98	2	-15.23 ±0.11	1	-11.14±1.93
	OPLS						
	OPC3		SPCE		TIP3P		
Molecule	$\Delta G_{calc.}$	N_g	$\Delta G_{calc.}$	N_g	$\Delta G_{calc.}$	N_g	$\Delta G_{\rm exp}$
2pro.	-3.53 ±0.17	2	-3.46 ±0.18	2	-3.52 ±0.09	2	-6.40±0.60
acet.	-10.66 ±0.31	2	-10.66 ±0.18	3	-11.35 ±0.25	2	-9.94±0.18
cycl.	-4.37 ±0.11	1	-4.40 ±0.09	1	-4.15 ±0.06	1	-4.59±0.60
dial.	-23.55 ±0.43	1	-23.47 ±0.43	1	-24.03 ±0.18	2	-5.74±1.93
keto.	-10.75 ±0.19	1	-10.77 ±0.13	1	-11.78 ±0.09	1	-10.78±0.18
nitr.	-12.98 ±0.25	1	-13.13 ±0.14	1	-14.13 ± 0.10	1	-7.98±1.93
prof.	-7.12 ±0.28	1	-7.62 ±0.21	1	-8.49 ±0.13	1	-2.45±1.37
terb.	-10.94 ±0.18	1	-10.97 ±0.12	1	-11.33 ±0.08	1	-11.14±1.93

In the Figure 6, the calculated free energies of Table 3 are reported against the experimental data.

Figure 6: Left panel: correlation diagram for calculated (GAFF2) and experimental solvation free energies in water. Right panel: same with OPLS-AA. The green squares refer to the calculated hydration free energies reported in Ref.[19] done with GAFF1 and FEP. The gray shaded area includes the points with computed free energies differing by less than 2.5 kcal mol^{-1} with respect to the experimental data. For methodological (FSAM) errors on the computed data see Table 3.

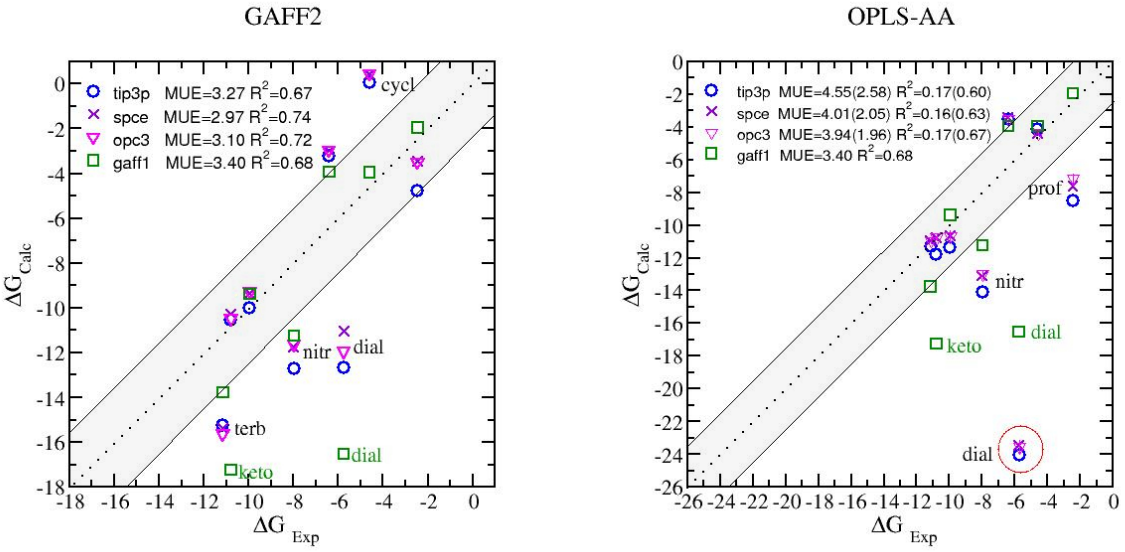

We first notice that the main differences in the computed values are due to the force fields, with the adopted water model having a limited impact on the hydration free energgy. If we compute the R^2 Pearson coefficient, the slope a and the intercept b of the regression line for the OPLS-AA and GAFF2 datasets, we find in fact similar results for all three water model, namely $R^2 = 0.69$, $a = 0.79$, $b = -4.04$ for OPC3, $R^2 = 0.66$, $a = 0.76$, $b = -4.48$ for SPCE and $R^2 = 0.74$, $a = 0.89$, $b = -3.41$ for TIP3P. The TIP3P model, in most cases, predicts a slightly lower hydration free energy. This is due to the systematic underestimation of the solute cavity work (see Figure 4, right panel) induced by the lower density of the TIP3P liquid in standard conditions (see Table 1).

The agreement with experimental data, although acceptable, is somewhat below expectations for both OPLS-AA and GAFF2 force fields.

GAFF2/SPCE, on the overall, seems to perform slightly better than all other combinations as far as the mean unsigned error (MUE) and the correlation coefficient R^2 are

concerned. For cyclohexanamine, however, the predicted values of the GAFF/SPCE combination is nearly 5 kcal mol^{-1} off the experimental counterpart and in only three cases (prof, keto, acet) GAFF2/SPCE or GAFF2/OPC3 exhibits hydration free energy differing by less than 1 kcal with respect to the experimental value. Also the improvement with respect to GAFF1 (green square in Figure 6) is moderate, with definitely better results for keto and dialifor, but with degradation in other cases, such as cyclohexanamine.

The MUE and R^2 for the OPLS-AA are strongly affected by the predicted hydration free energy for dialifor which is nearly 20 kcal off the experimental value. This is due, as we have seen in Figure 4, to a much larger ΔG_q contribution in OPLS-AA dialifor with respect to GAFF2. If we eliminate the outlier dialifor, OPLS-AA MUE improves substantially, declining below 2 kcal mol^{-1} in combination with the OPC3 model. OPLS-AA/OPC3 has five compounds within the 2.5 kcal band, while GAFF/SPCE has only four. Since the OPLS-AA/GAFF2 ΔG_{LJ} dispersive-repulsive contribution are strongly correlated (see Figure 4 right), it follows that the underestimation and overestimation of the hydration free energy in cyclohexanamine (GAFF2) and in dialifor (OPLS-AA), respectively, is entirely due to the modeling of the atomic charges. OPLS-AA has higher charge strength with respect to GAFF2 for both cyclohexanamine and dialifor (see Table 2 and see the `tpgprm` provided as Supporting Information). However, if a large I_m on the amine group appears to be beneficial for cyclohexanamine, the large I_m, especially for the SO_2P_2 group, in OPLS-AA dialifor produces unrealistic values of the hydration free energy.

In Table 4 we conclude this section by reporting the computed solvation free energies in 1-octanol of the eight molecules using the GAFF2 and OPLS-AA parameterization. The table include the ADT A^2 value and the number of components of the work distributions in 1-octanol (reported in the Figure 7 further on).

Table 4: Solvation free energies (kcal mol^{-1}) in 1-octanol obtained with OPLS-AA and GAFF2. The error has been calculated using bootstrap with resampling.[66]

	GAFF			OPLS		
mol	ΔG	A^2	N_g	ΔG	A^2	N_g
2pro	-4.82± 0.15	0.22	1	-4.73 ± 0.09	4.47	2
acet	-11.44± 0.34	0.37	1	-11.58 ± 0.41	0.57	1
cycl	-4.36± 0.11	0.47	1	-5.46 ± 0.13	0.15	1
dial	-20.07± 0.42	0.52	1	-25.47 ± 0.85	0.39	1
keto	-15.12± 0.50	0.15	1	-16.34 ± 0.41	0.39	1
nitr	-19.79± 0.50	0.23	1	-18.83 ± 0.44	0.30	1
prof	-14.12± 0.26	0.27	1	-14.95 ± 0.32	0.51	1
terb	-18.64± 0.40	0.64	1	-16.79 ± 0.28	0.27	1

For this mostly hydrophobic solvent, OPLS-AA, GAFF2 appears to deliver similar values of the solvation free energies. The OPLS-AA/GAFF2 Pearson correlation coefficient yields $R^2 = 0.95$ with slope and intercept given by $a = 1.04$ and $b = 0.10$, respectively.

Partition coefficients

Previous results have shown that the adopted water model has a limited impact on the hydration free energies. OPC3 and SPCE turned out to perform slightly better than TIP3P for both OPLS-AA and GAFF2 (see Table 4). In computing the partition coefficient we have hence selected the hydration free energies obtained with the OPC3 water model for both OPLS-AA and GAFF2.

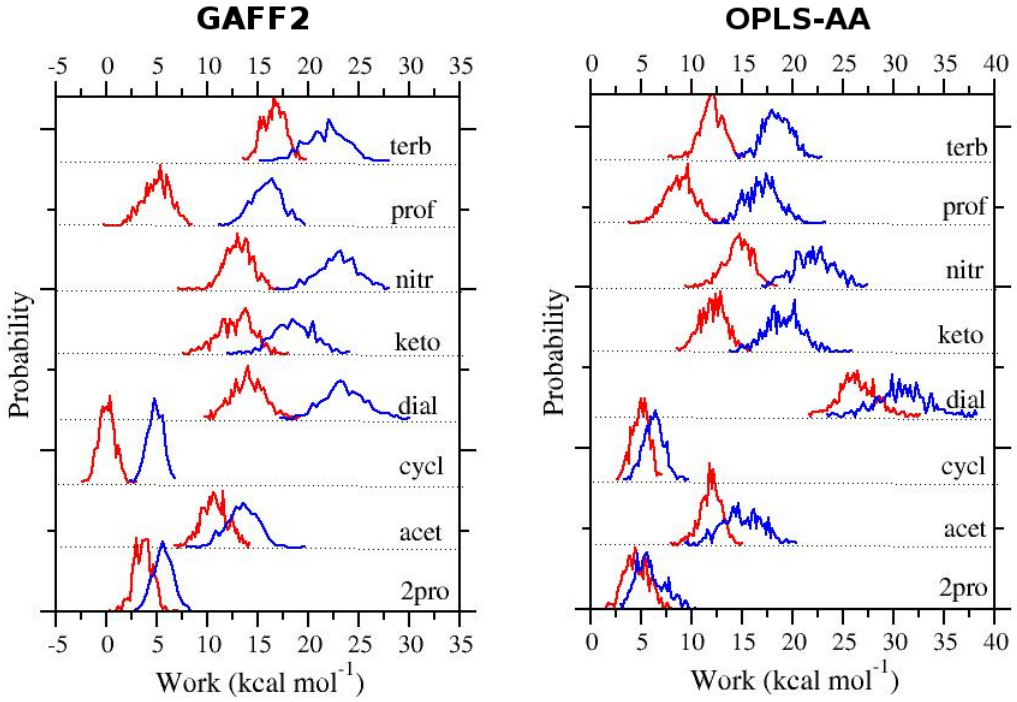

Figure 7: Work distribution for the annihilation of the solute in water (red color) and 1-octanol (blue color) using OPLS-AA (right panel) and GAFF2 (left panel). The parameterization of the solvent molecule in 1-octanol is provided by the GAFF2 and OPLS-AA automatic parameter generators, PrimaDORAC and LigParGen, respectively. For water, the OPC3 model was used in both cases.

Figure 7 collects the work distributions obtained in the annihilation of the eight solute molecules in 1-octanol (blue color) and in OPC3 water, using either OPLS-AA or GAFF. We can see, in general, that the solvation free energy is higher in 1-octanol than in OPC3 water for both force fields, translating in *positive* o/w partition coefficients. The latter can be in fact defined as

$$\mathrm{LogP} = -\frac{\Delta G_{\mathrm{oct}} - \Delta G_{\mathrm{opc3}}}{RT \ln 10} \tag{3}$$

The LogP coefficients for the eight solutes and the two force fields are collected in Table 5. The reported errors are given by $(RT \ln 10)^{-1}$ times the sum of the bootstrap errors on ΔG_{oct} and ΔG_{opc3} (see Table 4 and Table 3, respectively). The experimental LogP are taken, in all cases, from the PUBCHEM database.[21] For nitralin, experimental LogP is unavailable and the xLogp3 value[67] is used. The two force fields correctly predict positive LogP for

all solutes. In general, discrepancies with respect to the experimental data appears to be less important with respect to those observed for the hydration free energy (see Table 3 and Figure 4), apparently showing a compensation error effect when evaluating $\Delta\Delta G$ differences.

Table 5: Computed and experimental[21] LogP partition coefficient for the eight selected molecules using GAFF2 and OPLS-AA. The water solvent model used in the computed LogP is OPC3 for both OPLS-AA and GAFF2.

mol	LogP		LogP(Exp)
	GAFF	OPLS	
2pro	1.36± 0.20	0.88± 0.19	0.08
acet	1.57± 0.44	0.67± 0.53	1.19
cycl	3.50± 0.14	0.80± 0.17	1.49
dial	5.92± 0.46	1.40± 0.93	4.89
keto	3.38± 0.68	4.08± 0.44	3.12
nitr	5.95± 0.52	4.27± 0.51	3.7
prof	7.76± 0.36	5.72± 0.44	5.58
terb	2.19± 0.41	4.27± 0.33	1.89

The comparison of computed and experimental LogP can be best appreciated in Figure 8 that somehow represents a summa of our study. On the overall, again GAFF2 appears to perform better than OPLS-AA. However, the MUE and R^2 values of the latter force filed are strongly affected by the single LogP value of dialifor. We recall that the ΔG_{opc3} for dialifor was found to differ by nearly 20 kcal mol^{-1} with respect to the experimental hydration free energy, due to an excessive charge molecular strength, I_m. Error compensation in dialifor OPLS-AA, while correctly producing a positive LogP, was apparently unable to recover the experimental outcome, yielding an underestimation of LogP by more than 3 units. If we eliminate the outlier dialifor, OPLS-AA MUE drops below 1 units. As shown in the Figure 8, remarkably OPLS-AA has six molecules (2pro, acet, cycl, keto, nitr, prof) yielding a $\Delta\Delta G$ differing by less than 1 kcal mol^{-1} with respect to the experimental value. GAFF2, on the other hand, has 5 molecules (2pro, acet, terb, keto, dialifor) yielding differences between experimental and computed values of less than 1.5 kcal mol^{-1}.

Figure 8: Correlation diagram of computed and experimental LogP o/w partition coefficient. Experimental LogP value are taken from the PUBCHEM database.[21] For Nitralin, only the XLogp3 value is provided in PUBCHEM. For data points within the shaded band, the water octanol solvation free energy difference is within 1 kcal mol^{-1} of the experimental value.

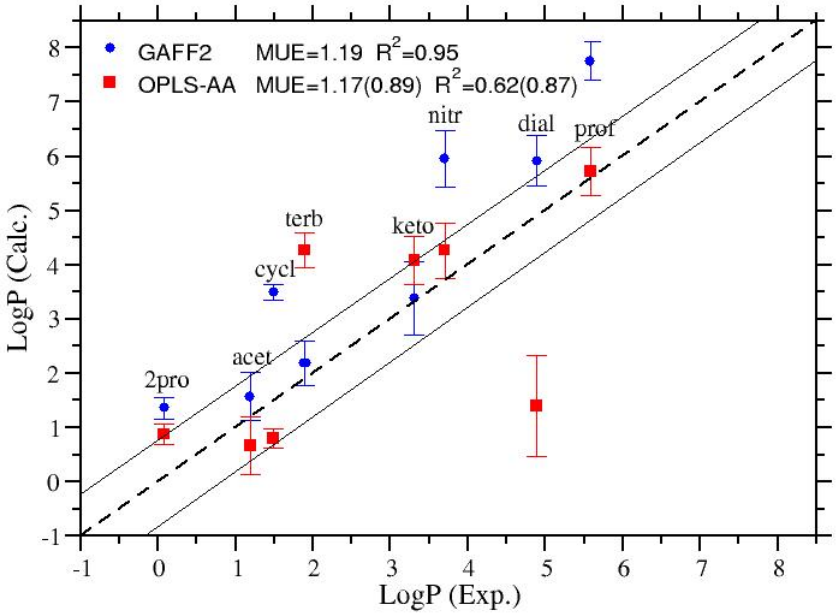

The relatively low MUE's for the two force fields translate into $\Delta\Delta G$ mean unsigned errors of less than 1.5 kcal mol^{-1} which is indeed a remarkable accuracy for parameterizations based on transferable and general force field and that were automatically generated. In this regard, it should be stressed that LogP, or equivalently $\Delta\Delta G$ values, are especially relevant for binding free energy calculations in drug-receptor systems.

Conclusion

In this paper we have computed the hydration free energies and the octanol/water partition coefficients for eight selected organic molecules characterized by a complex conformational landscape and/or by the presence of disparate chemical moieties. Computation have been done using the two popular general force fields OPLS and GAFF, in their recently released

variants (OPLS-AA, GAFF2). Parameterization of each of the eight molecules was generated automatically using LigParGen[14] for OPLS-AA and PrimaDORAC[15] for GAFF2. The hydration free energies were evaluated using three different water models (OPC3, SPCE and TIP3P), hence producing a total of 48 calculations. 1-octanol was modeled using LigParGen (OPLS-AA) and PrimaDORAC (GAFF2) parameterization, for a total of 16 solvation free energy calculations. All solvation free energies were determined using the recently developed fast switching annihilation method, FSAM.[25] The methodology relies on two main computational steps, consisting in the canonical sampling of fully coupled solute conformations using efficient enhanced sampling techniques and, starting form these states, in the subsequent fast decoupling of the solute in a collection of driven NE trajectories. The decoupling free energies (equal to minus the solvation free energies) are recovered from the nonequilibrium work distributions using unbiased estimates solidly banking on the Crooks non equilibrium theorem.[53] FSAM, along with the free energy estimate, by design provides a straightforward and highly reliable confidence interval from a *single* work distribution,[47] with no need for checking, a posteriori or on the fly,[68] the balance of the variances in equilibrium stratification (FEP-based) techniques.[56]

As a general trend, common to all selected solutes, we have seen that in water the quantity ΔG_q and ΔG_{LJ}, i.e. the discharging and the dispersive-repulsive contributions to the decoupling free energy, have opposite signs, while in 1-octanol both these contribution are positive. Hydration free energies have been found rather insensitive to the adopted water model. We found that the TIP3P model, due to the underestimation of the density of the liquid, consistently yields ΔG_{LJ} that are smaller than those obtained with OPC3 and SPCE.

Agreement with experimental hydration free energies is acceptable for both force fields, but with difference between experimental and calculated values in most cases largely exceeding the FSAM uncertainty. GAFF2 exhibits a moderate improvement with respect to GAFF1.[19] On the overall, GAFF2/SPCE resulted the best combination for hydration free energies for the eight selected compounds, yielding a mean unsigned around 3 kcal mol^{-1}.

By eliminating the outlier dialifor, OPLS-AA/OPC3 becomes the best alternative for the remaining solutes with a mean unsigned error dropping to less than 2 kcal mol^{-1}. Discrepancies in the solvation free energies stem from the electrostatic part of the force field, since OPLS-AA and GAFF2 produce similar ΔG_{LJ} values. This is somehow encouraging in perspective force field refinement studies, since the dispersive-repulsive contribution is essentially controlled by the mean shape of molecule in solution and by the Lennard-Jones potential, i.e. by the *transferable* part of the general force field, relying on the definition of a restricted set of *atom types*. Our results hence indicate that most of the effort for general force field improvement should be invested on the non transferable electrostatic part of the force field, by adjusting and tuning the available atomic charge calculation protocols, namely AM1/BCC for GAFF2 and 1.14*CM1A or 1.14*CM1A-LBCC for OPLS-AA.

When computing the octanol/water partition coefficient LogP, OPLS-AA and GAFF2 force fields perform better due to an error compensation effect. Error compensation can be easily explained by considering that the major source of error is due to the ΔG_q discharging contribution and that the error in ΔG_q has the same sign in both solvent. MUE's on the LogP values have been found around one unity, hence implying a mean deviation of the $\Delta\Delta G$ values within 1.5 kcal mol^{-1}. This small error has been obtained on a set of organic molecules coarsely spanning a significant portion of the chemical space and characterized by the presence of multiple rotable bonds. It should also be stressed that these results were obtained by using "as is" the parameterizations provided by web-based automatic parameter generator based on these force field, namely PrimaDORAC for GAFF2 and LigParGen for OPLS-AA, hence convincingly validating these tools for scientific applications. On the overall our study is indeed encouraging for perspective binding free energy calculations in drug discovery projects.

Acknowledgement

We acknowledge the Partnership for Advance Computing in Europe (PRACE) for awarding us access to Marconi-Broadwell and Marconi-KNL HPC platforms managed by the CINECA consortium (Italy). A part of the computing resources and the related technical support used for this work have been provided by CRESCO/ ENEAGRID HPC infrastructure and its staff.[58]

Supporting Information Available

Equilibrium conformational data from the HREM-TT stage. Gaussian estimate as a function of the annihilation time. Full work distribution data. Computed and experimental partition/coefficient data. Compresses archive containing the topological and parameter files of all chemical species (solute and solvents)

References

(1) Drug Design Data Resource (D3R), SAMPL6: Host-guest binding and physical property prediction. Information available at https://drugdesigndata.org/about/sampl (accessed 15 October 2018); Full free energy data available at https://drugdesigndata.org/upload/community-components/d3r/workshop2018/presentations/DavidMobley2018_SAMPL_overview.pdf (accessed 15 October 2018).

(2) Yin, J.; Henriksen, N. M.; Slochower, D. R.; Shirts, M. R.; Chiu, M. W.; Mobley, D. L.; Gilson, M. K. Overview of the SAMPL5 host–guest challenge: Are we doing better? *J. of Comput. Aided Mol. Des.* **2016**, 1–19.

(3) Muddana, H. S.; Fenley, A. T.; Mobley, D. L.; Gilson, M. K. The SAMPL4 host–guest blind prediction challenge: an overview. *J. Comput. Aided Mol. Des.* **2014**, *28*, 305–317.

(4) Chodera, J.; Mobley, D.; Shirts, M.; Dixon, R.; K.Branson,; Pande, V. Alchemical free energy methods for drug discovery: progress and challenges. *Curr. Opin. Struct. Biol* **2011**, *21*, 150–160.

(5) Gumbart, J. C.; Roux, B.; Chipot, C. Standard Binding Free Energies from Computer Simulations: What Is the Best Strategy? *J. Chem. Theory Comput.* **2013**, *9*, 974–802.

(6) Hansen, N.; van Gunsteren, W. F. Practical Aspects of Free-Energy Calculations: A Review. *J. Chem. Teory Comput.* **2014**, *10*, 2632–2647.

(7) Wang, L.; Wu, Y.; Deng, Y.; Kim, B.; Pierce, L.; Krilov, G.; Lupyan, D.; Robinson, S.; Dahlgren, M. K.; Greenwood, J.; Romero, D. L.; Masse, C.; Knight, J. L.; Steinbrecher, T.; Beuming, T.; Damm, W.; Harder, E.; Sherman, W.; Brewer, M.; Wester, R.; Murcko, M.; Frye, L.; Farid, R.; Lin, T.; Mobley, D. L.; Jorgensen, W. L.; Berne, B. J.; Friesner, R. A.; Abel, R. Accurate and Reliable Prediction of Relative Ligand Binding Potency in Prospective Drug Discovery by Way of a Modern Free-Energy Calculation Protocol and Force Field. *J. Am. Chem Soc.* **2015**, *137*, 2695–2703.

(8) DeVivo, M.; Masetti, M.; Bottegoni, G.; Cavalli, A. Role of Molecular Dynamics and Related Methods in Drug Discovery. *J. Med. Chem.* **2016**, *59*, 4035–61.

(9) Procacci, P. Alchemical determination of drug-receptor binding free energy: Where we stand and where we could move to. *J. Mol. Graph. and Model.* **2017**, *71*, 233–241.

(10) Wang, J.; Wolf, R.; Caldwell, J.; Kollman, P.; Case, D. Development and testing of a general AMBER force field. *J. Comp. Chem.* **2004**, *25*, 1157–1174.

(11) Dodda, L. S.; Vilseck, J. Z.; Tirado-Rives, J.; Jorgensen, W. L. 1.14*CM1A-LBCC:

Localized Bond-Charge Corrected CM1A Charges for Condensed-Phase Simulations. *J. Phys. Chem. B* **2017**, *121*, 3864–3870.

(12) Vanommeslaeghe, K.; Hatcher, E.; Acharya, C.; Kundu, S.; Zhong, S.; Shim, J.; Darian, E.; Guvench, O.; Lopes, P.; Vorobyov, I.; Mackerell, A. D. CHARMM general force field: A force field for drug-like molecules compatible with the CHARMM all-atom additive biological force fields. *J. Comput. Chem. 31*, 671–690.

(13) GAFF and GAFF2 are public domain force fields and are part of the AmberTools16 distribution, available for download at http://amber.org internet address (accessed October 2018). According to the AMBER development team, the improved version of GAFF, GAFF2, is an ongoing poject aimed at "reproducing both the high quality interaction energies and key liquid properties such as density, heat of vaporization and hydration free energy". GAFF2 is expected "to be an even more successful general purpose force field and that GAFF2-based scoring functions will significantly improve the successful rate of virtual screenings.".

(14) Dodda, L. S.; Cabeza de Vaca, I.; Tirado-Rives, J.; Jorgensen, W. L. LigParGen web server: an automatic OPLS-AA parameter generator for organic ligands. *Nucleic Acids Res.* **2017**, *45*, W331–W336.

(15) Procacci, P. PrimaDORAC: A Free Web Interface for the Assignment of Partial Charges, Chemical Topology, and Bonded Parameters in Organic or Drug Molecules. *J. Chem. Inf. Model.* **2017**, *57*, 1240–1245.

(16) Jorgensen, W. L.; Buckner, J. K.; Boudon, S.; TiradoRives, J. Efficient computation of absolute free energies of binding by computer simulations. Application to the methane dimer in water. *J. Chem Phys.* **1988**, *89*, 3742–3746.

(17) Gilson, M. K.; Given, J. A.; Bush, B. L.; McCammon, J. A. The Statistical-

Thermodynamic Basis for Computation of Binding Affinities: A Critical Review. *Biophys. J.* **1997**, *72*, 1047–1069.

(18) Procacci, P.; Chelli, R. Statistical Mechanics of Ligand-Receptor Noncovalent Association, Revisited: Binding Site and Standard State Volumes in Modern Alchemical Theories. *J. Chem. Theory Comput.* **2017**, *13*, 1924–1933.

(19) Mobley, D. L.; Guthrie, J. P. FreeSolvq: a database of experimental and calculated hydration free energies, with input files. *J. Comput.-Aided Mol. Des.* **2014**, *28*, 711–720.

(20) Wishart, D. S.; Feunang, Y. D.; Guo, A. C.; Lo, E. J.; Marcu, A.; Grant, J. R.; Sajed, T.; Johnson, D.; Li, C.; Sayeeda, Z.; Assempour, N.; Iynkkaran, I.; Liu, Y.; Maciejewski, A.; Gale, N.; Wilson, A.; Chin, L.; Cummings, R.; Le, D.; Pon, A.; Knox, C.; Wilson, M. DrugBank 5.0: a major update to the DrugBank database for 2018. *Nucleic Acids Res.* **2018**, *46*, D1074–D1082.

(21) Kim, S.; Thiessen, P. A.; Bolton, E. E.; Chen, J.; Fu, G.; Gindulyte, A.; Han, L.; He, J.; He, S.; Shoemaker, B. A.; Wang, J.; Yu, B.; Zhang, J.; Bryant, S. H. PubChem Substance and Compound databases. *Nucleic Acids Res.* **2016**, *44*, D1202–D1213.

(22) Jorgensen, W. L.; Chandrasekhar, J.; Madura, J. D.; Impey, R. W.; Klein, M. L. Comparison of simple potential functions for simulating liquid water. *J. Chem. Phys.* **1983**, *79*, 926–935.

(23) Kusalik, P. G.; Svishchev, I. M. The spatial structure in liquid water. *Science* **1994**, *265*, 1219–1221.

(24) Izadi, S.; Onufriev, A. V. Accuracy limit of rigid 3-point water models. *J. Chem. Phys.* **2016**, *145*, 074501.

(25) Procacci, P.; Cardelli, C. Fast Switching Alchemical Transformations in Molecular Dynamics Simulations. *J. Chem. Theory Comput.* **2014**, *10*, 2813–2823.

(26) Sandberg, R. B.; Banchelli, M.; Guardiani, C.; Menichetti, S.; Caminati, G.; Procacci, P. Efficient Nonequilibrium Method for Binding Free Energy Calculations in Molecular Dynamics Simulations. *J. Chem. Theory Comput.* **2015**, *11*, 423–435.

(27) Zwanzig, R. W. High-temperature equation of state by a perturbation method. I. Nonpolar gases. *J. Chem. Phys.* **1954**, *22*, 1420–1426.

(28) Kirkwood, J. G. Statistical mechanics of fluid mixtures,. *J. Chem. Phys.* **1935**, *3*, 300–313.

(29) Sugita, Y.; Okamoto, Y. Replica-exchange molecular dynamics method for protein folding. *Chem. Phys. Lett.* **1999**, *314*, 141–151.

(30) Park, S.; Schulten, K. Calculating potentials of mean force from steered molecular dynamics simulations. *J. Chem. Phys.* **2004**, *120*, 5946–5961.

(31) Procacci, P.; Marsili, S.; Barducci, A.; Signorini, G. F.; Chelli, R. Crooks equation for steered molecular dynamics using a Nosé-Hoover thermostat. *J. Chem. Phys.* **2006**, *125*, 164101.

(32) Procacci, P. Unbiased free energy estimates in fast nonequilibrium transformations using Gaussian mixtures. *J. Chem. Phys.* **2015**, *142*, 154117.

(33) Procacci, P. Hybrid MPI/OpenMP Implementation of the ORAC Molecular Dynamics Program for Generalized Ensemble and Fast Switching Alchemical Simulations. *J. Chem. Inf. Model.* **2016**, *56*, 1117–1121.

(34) Jakalian, A.; Jack, D. B.; Bayly, C. I. Fast, efficient generation of high-quality atomic charges. AM1-BCC model: II. Parameterization and validation. *J. Comput. Chem.* **2002**, *23*, 1623–1641.

(35) Mobley, D. L.; Bayly, C. I.; Cooper, M. D.; Shirts, M. R.; Dill, K. A. Small Molecule Hydration Free Energies in Explicit Solvent: An Extensive Test of Fixed-Charge Atomistic Simulations. *J. Chem. Teory Comput.* **2009**, *5*, 350–358.

(36) Abraham, M. J.; Murtola, T.; Schulz, R.; Páll, S.; Smith, J. C.; Hess, B.; Lindahl, E. GROMACS: High performance molecular simulations through multi-level parallelism from laptops to supercomputers. *SoftwareX* **2015**, *1-2*, 19–25.

(37) Salomon-Ferrer, R.; Case, D. A.; Walker, R. C. An overview of the Amber biomolecular simulation package. *Wiley Interdisciplinary Reviews: Computational Molecular Science* **2013**, *3*, 198–210.

(38) Weininger, D. SMILES, a chemical language and information system. 1. Introduction to methodology and encoding rules. *J. Chem. Inf. Comput. Sci.* **1988**, *28*, 31–36.

(39) O'Boyle, N. M.; Banck, M.; James, C. A.; Morley, C.; Vandermeersch, T.; Hutchison, G. R. Open Babel: An open chemical toolbox. *J. Cheminf.* **2011**, *3*, 33.

(40) Marchi, M.; Procacci, P. Coordinates scaling and multiple time step algorithms for simulation of solvated proteins in the NPT ensemble. *J. Chem. Phys.* **1998**, *109*, 5194–520g2.

(41) Tuckerman, M.; Berne, B. J. Reversible multiple time scale molecular dynamics. *J. Chem. Phys.* **1992**, *97*, 1990–2001.

(42) Procacci, P.; Paci, E.; Darden, T.; Marchi, M. ORAC: A Molecular Dynamics Program to Simulate Complex Molecular Systems with Realistic Electrostatic Interactions. *J. Comput. Chem.* **1997**, *18*, 1848–1862.

(43) Essmann, U.; Perera, L.; Berkowitz, M. L.; Darden, T.; Lee, H.; Pedersen, L. G. A smooth particle mesh Ewald method. *J. Chem. Phys.* **1995**, *103*, 8577–8593.

(44) Procacci, P. I. Dissociation free energies of drug-receptor systems via non-equilibrium alchemical simulations: a theoretical framework. *Phys. Chem. Chem. Phys.* **2016**, *18*, 14991–15004.

(45) Nerattini, F.; Chelli, R.; Procacci, P. II. Dissociation free energies in drug-receptor systems via nonequilibrium alchemical simulations: application to the FK506-related immunophilin ligands. *Phys. Chem. Chem. Phys.* **2016**, *18*, 15005–15018.

(46) Procacci, P. Myeloid Cell Leukemia 1 Inhibition: An in Silico Study Using Non-equilibrium Fast Double Annihilation Technology. *J. Chem. Teory Comput.* **2018**, *14*, 3890–3902.

(47) Procacci, P.; Guarrasi, M.; Guarnieri, G. SAMPL6 host–guest blind predictions using a non equilibrium alchemical approach. *J. Comput.-Aided Mol. Des.* **2018**,

(48) Marsili, S.; Signorini, G. F.; Chelli, R.; Marchi, M.; Procacci, P. ORAC: A Molecular Dynamics Simulation Program to Explore Free Energy Surfaces in Biomolecular Systems at the Atomistic Level. *J. Comput. Chem.* **2010**, *31*, 1106–1116.

(49) Cardelli, C.; Barducci, A.; Procacci, P. Lipid tempering simulation of model biological membranes on parallel platforms. *BBA-Biomembranes* **2018**, *1860*, 1480 – 1488.

(50) Anderson, T. W.; Darling, D. A. A test of goodness of fit. *J. Am. Stat. Ass.* **1954**, *49*, 765–769.

(51) Stephens, M. Test of fit for the logistic distribution based on the empirical distribution function. *Biometrika* **1979**, *66*, 591–595.

(52) Razali, N. M.; Wah, Y. B. Power comparisons of Shapiro-Wilk, Kolmogorov-Smirnov, Lilliefors and Anderson-Darling tests. *J. Stat. Model. Anal.* **2011**, *2*, 21–33.

(53) Crooks, G. E. Nonequilibrium measurements of free energy differences for microscopically reversible Markovian systems. *J. Stat. Phys.* **1998**, *90*, 1481–1487.

(54) Sindhikara, D.; Meng, Y.; Roitberg, A. E. Exchange frequency in replica exchange molecular dynamics. *J. Chem. Phys.* **2008**, *128*, 024103.

(55) Consorzio Interuniversitario del Nord est Italiano Per il Calcolo Automatico (Interuniversity Consortium High Performance Systems) http://www.cineca.it (accessed 15 October 2018).

(56) Pohorille, A.; Jarzynski, C.; Chipot, C. Good Practices in Free-Energy Calculations. *J. Phys. Chem. B* **2010**, *114*, 10235–10253.

(57) Beutler, T.; Mark, A.; van Schaik, R.; Gerber, P.; van Gunsteren, W. Avoiding singularities and numerical instabilities in free energy calculations based on molecular simulations. *Chem. Phys. Lett.* **1994**, *222*, 5229–539.

(58) Ponti, G.; Palombi, F.; Abate, D.; Ambrosino, F.; Aprea, G.; Bastianelli, T.; Beone, F.; Bertini, R.; Bracco, G.; Caporicci, M.; Calosso, B.; Chinnici, M.; Colavincenzo, A.; Cucurullo, A.; Dangelo, P.; De Rosa, M.; De Michele, P.; Funel, A.; Furini, G.; Giammattei, D.; Giusepponi, S.; Guadagni, R.; Guarnieri, G.; Italiano, A.; Magagnino, S.; Mariano, A.; Mencuccini, G.; Mercuri, C.; Migliori, S.; Ornelli, P.; Pecoraro, S.; Perozziello, A.; Pierattini, S.; Podda, S.; Poggi, F.; Quintiliani, A.; Rocchi, A.; Scio, C.; Simoni, F.; Vita, A. *Proceeding of the International Conference on High Performance Computing & Simulation*; Institute of Electrical and Electronics Engineers (IEEE), 2014; pp 1030–1033.

(59) CRESCO: Centro computazionale di RicErca sui Sistemi COmplessi. Italian National Agency for New Technologies, Energy (ENEA), See `https:/http://www.cresco.enea.it` (accessed 15 October 2018).

(60) Jarzynski, C. Nonequilibrium equality for Free energy differences. *Phys. Rev. Lett.* **1997**, *78*, 2690–2693.

(61) Hummer, G. Fast-growth thermodynamic integration: Error and efficiency analysis. *J. Chem. Phys.* **2001**, *114*, 7330–7337.

(62) Shirts, M. R.; Pande, V. S. Comparison of efficiency and bias of free energies computed by exponential averaging, the Bennett acceptance ratio, and thermodynamic integration. *J. Chem. Phys.* **2005**, *122*, 144107.

(63) Oberhofer, H.; Dellago, C.; Geissler, P. L. Biased Sampling of Nonequilibrium Trajectories: Can Fast Switching Simulations Outperform Conventional Free Energy Calculation Methods? *J. Phys. Chem. B* **2005**, *109*, 6902–6915.

(64) Farrell, P. J.; Rogers-Stewart, K. Comprehensive study of tests for normality and symmetry: extending the Spiegelhalter test. *J. Stat. Comput. Sim.* **2006**, *76*, 803–816.

(65) Dempster, A.; Laird, N.; Rubin, D. Maximum Likelihood from Incomplete Data via the EM Algorithm. *J. Royal Stat. Soc. B* **1977**, *39*, 1–38.

(66) Putter, H.; Zwet, W. R. V. Resampling: Consistency of Substitution Estimators. *Ann. Stat.* **1996**, *24*, 2297–2318.

(67) Cheng, T.; Zhao, Y.; Li, X.; Lin, F.; Xu, Y.; Zhang, X.; Li, Y.; Wang, R.; Lai, L. Computation of Octanol-Water Partition Coefficients by Guiding an Additive Model with Knowledge. *J. Chem. Inf. Model.* **2007**, *47*, 2140–2148.

(68) Hahn, A. M.; Then, H. Characteristic of Bennett's acceptance ratio method. *Phys. Rev. E* **2009**, *80*, 031111.

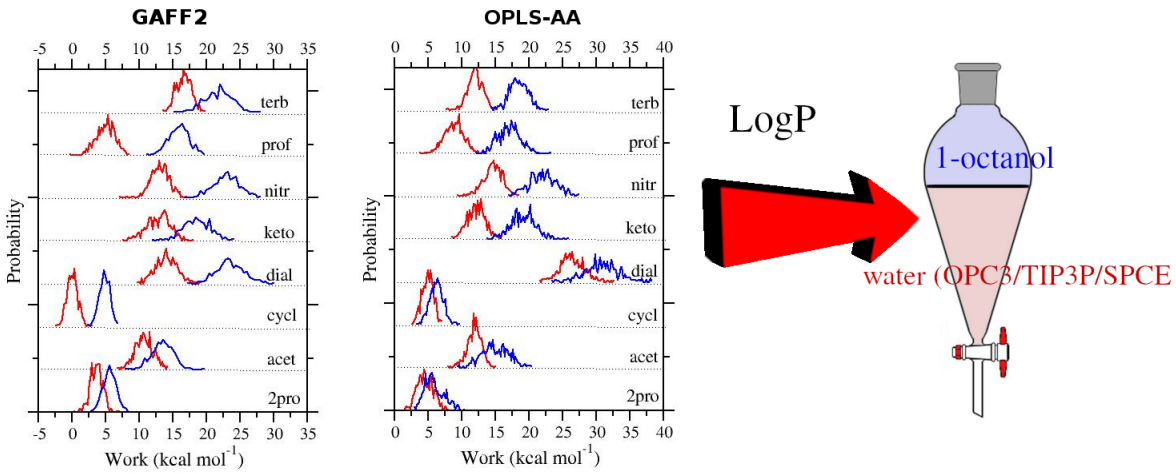
GAFF2
OPLS-AA
Probability
Work (kcal mol-1)
terb
prof
nitr
keto
dial
cycl
acet
2pro
LogP
1-octanol
water (OPC3/TIP3P/SPCE